



A fast modelling tool for plate heat exchangers based on depth-averaged equations

Marko Lyytikäinen*, Taija Hämäläinen, Jari Hämäläinen

Department of Physics, University of Kuopio, P.O. Box 1627, FIN-70211 Kuopio, Finland

ARTICLE INFO

Article history:

Received 14 March 2008

Received in revised form 19 August 2008

Available online 5 November 2008

Keywords:

Plate heat exchanger

CFD

Depth-averaging

Pressure drop

Temperature change

ABSTRACT

In this study, the depth-averaged flow and energy equations for plate heat exchangers are presented. The equations are derived by integrating the original 3D flow and energy equations over the height of the gap between the bottom and top plates. This approach reduces the equations from 3D to 2D but still takes into account the frictions on the surfaces and heat transfer through the plates. The depth-averaging reduces the elapsed time of CFD simulations from hours to minutes. Thus, it is very practicable modelling method in real time design work. 2D CFD simulations with depth-averaged equations are compared with full 3D models for five different corrugation angles and corrugation lengths. The simulation results show that the 2D model predicts with relatively good accuracy the profile of the pressure drop and the temperature change as a function of the corrugation angle and the function of the corrugation length. In order to get more extensive information about the significance of the different geometry parameters on the efficiency of the heat exchanger, we simulated 30 different geometries with the fast 2D model. The results suggest that the temperature change is not as sensitive for the geometrical modifications as the pressure drop.

© 2008 Elsevier Ltd. All rights reserved.

1. Introduction

Increasing needs to reduce energy costs emphasize the efficiency aspects in the heat exchanger design process. The most common type of heat exchangers are plate heat exchangers, in which plates are used to separate the hot and cold fluids. Thus, the design of the plate surface is the key issue when aiming to maximize the heat transfer. Nevertheless, the pressure drop has to be taken into account as well because it is one important factor affecting energy losses when pumping water in the heat exchanger. Both the pressure drop and the heat transfer coefficient are determined by the flow conditions, especially turbulence.

Most of the recent research on heat exchangers has focused on different correlations between the Nusselt number and the friction factor, because these quantities can be determined experimentally over the whole heat exchanger, i.e., globally [7]. The pressure drop and temperature change for multiple gap plate heat exchangers depend partly on the flow distribution to the channels from the conduit. The equations describing the flow distribution and pressure drop in plate heat exchangers have been derived analytically [2,3]. These equations agree well with experimental results for small and large plate packages, which shows how the pressure distribution between the first and the last channel is more uneven for larger plate packages [4,5]. Temperatures, heat loads and pressure drops, and also their distributions

using a few channels and flat plates have been analyzed with computational fluid dynamics (CFD) [6]. However, in our research the effect of maldistribution need not be taken into account, because only the dependence of the pressure drop and heat transfer on the channel geometry is studied. Flow phenomena and heat transfer rate have been analyzed globally and locally with CFD based modelling, giving invaluable information about the effect of geometrical details on heat transfer rate and on friction losses for the design work [8]. The small scale effects of corrugation on heat transfer rate and friction losses have been studied by simulating a few corrugation cycles using the side profile of the channel [9].

However, when determining the dependence of the heat transfer rate and pressure losses on geometry parameters in the product development process, efficiency analysis of a whole single plate with dozens of different parameter combinations is needed. In addition, the pre-processing, i.e., generating geometry and mesh, is a very complicated and time consuming part of the whole development process, because it has to be done for every geometry. Therefore, simplifications are needed in order to make modelling faster for a real design process. This can be accomplished by using depth-averaged equations for flow and heat transfer modelling. These equations are derived by integrating the original 3D flow and energy equations over the height of the gap between the bottom and top plates. This approach reduces the equations from 3D to 2D but still takes into account the frictions on the surfaces, height of the channel and heat transfer through the plates. Even though some of the 3D flow structures are lost, this approach

* Corresponding author. Tel.: +358 17163076; fax: +358 17162585.
E-mail address: Marko.Lyytikainen@uku.fi (M. Lyytikäinen).

Nomenclature

D	channel's depth	S	velocity profile
S_m	source term of mass	c_f	bed friction coefficient
P_{kv}	source of turbulence kinetic energy	u_f	friction velocity
P_{ev}	source of dissipation	e	specific internal energy
γ	expansion coefficient of plate area	P	at point P
y^*	non-dimensional distance	Pr_t	turbulent Prandtl number
κ	von Kármán constant	E	empirical constant
y_T^*	non-dimensional thermal sublayer thickness	y_P	distance from point P to the wall
Δp	pressure drop	$\frac{\Delta T^*}{\Delta \bar{T}}$	normalized temperature change
$\overline{\Delta p}$	average of pressure drops		average of temperature changes
Δp^*	normalized pressure drop		

describes the phenomena in the heat exchanger with relatively good accuracy and it can be used in real time design work.

This paper introduces the depth-averaged flow and energy equations for a plate heat exchanger. The goal of this approach is to reduce the elapsed time of CFD simulations from hours to minutes. The source terms for turbulence kinetic energy and its dissipation rate in the standard $k - \epsilon$ model are taken from [10]. While they specified the heat transfer coefficient empirically as a global constant, we determine it in every computational cell by using local flow properties. The equations are used for modelling the chevron-type heat exchanger, where the plate geometries are presented with sine functions that contain the most important geometry parameters: the corrugation angle, the corrugation length and the corrugation depth. With this approach we need to generate only one 2D mesh and can present the height of the plate gap in every horizontal position with the source terms in governing equations. Thus, we can skip geometry pre-processing work and need only change the parameters of the sine functions. In addition, modelling is much faster with a 2D mesh than with a 3D mesh.

2. Theory**2.1. Flow equations**

In the present study, heat exchanger modelling is done using depth averaged flow and energy equations with the commercial CFD software Fluent. The steady-state depth-averaged mass conservation law can be written as

$$\nabla \cdot (\rho \bar{u}) = -\frac{\rho}{D} \bar{u} \cdot \nabla D = S_m \quad (1)$$

in which D is the channel's depth, $\bar{u} = (\bar{u}, \bar{v})$ is the depth-averaged velocity vector and ρ is the density. The right hand side is defined as a source term S_m . The source term of mass appears also in the momentum equation that is required for flow modelling. Depth-averaging of the z-directional derivatives of the stress tensor in the 3D momentum equation leads to the following expression

$$\frac{1}{D} \int_0^D \frac{\partial}{\partial z} (\tau_{iz}) dz = \frac{1}{D} [\tau_{iz}(D) - \tau_{iz}(0)], \quad i = x, y, \quad (2)$$

where τ_{xz} and τ_{yz} are the friction forces on the bottom and the upper surfaces. Fluid is assumed to be flowing horizontally, that is, the velocity component $w = 0$. Horizontal velocity components u and v are defined with the help of the average velocities \bar{u} and \bar{v} , and the z-directional profile S in the following form

$$u(x, y, z) = \bar{u}(x, y) \cdot S(z), \quad (3)$$

$$v(x, y, z) = \bar{v}(x, y) \cdot S(z), \quad (4)$$

where

$$S(z) = \frac{n+1}{n} \left(1 - \left| 1 - \frac{2}{D} z \right|^n \right), \quad (5)$$

where $n = 7$ for turbulent flow. Therefore, the friction forces on the bottom and the top surfaces are

$$\tau_{xz} = \mu \frac{\partial u}{\partial z} = \mu \bar{u} \frac{\partial S}{\partial z} = -\frac{4\mu \bar{u}(n+1)}{D^2}, \quad (6)$$

$$\tau_{yz} = \mu \frac{\partial v}{\partial z} = \mu \bar{v} \frac{\partial S}{\partial z} = -\frac{4\mu \bar{v}(n+1)}{D^2}, \quad (7)$$

where μ is the dynamic viscosity. Now the 2D depth-averaged conservation law-of-momentum without the time derivative term can be written as

$$\nabla \cdot (\rho \bar{u} \bar{u}) = -\nabla p + \nabla \cdot (\bar{\tau}) + \bar{u} S_m - \frac{4\mu \bar{u}(n+1)}{D^2}, \quad (8)$$

where p is the pressure and $\bar{\tau}$ is the stress tensor.

Derived mass balance and momentum equations are sufficient for laminar flow cases, otherwise we need to simulate turbulence quantities. The simplified production terms for turbulence and its dissipation are from [10]. The production of turbulent energy due to wall friction for k and ϵ equations is included via the production terms

$$P_{kv} = \rho c_k \frac{u_f^3}{D}, \quad (9)$$

$$P_{ev} = \rho c_\epsilon \frac{u_f^4}{D^2}, \quad (10)$$

where the empirical parameters are

$$c_k = \frac{1}{c_f^{1/2}},$$

$$c_\epsilon = 3.6 \frac{c_{2\epsilon} c_\mu^{1/2}}{c_f^{3/4}},$$

where c_f

$$c_f = \frac{u_f^2}{u^2} \quad (11)$$

is the friction coefficient, u_f is the friction velocity, u is the velocity, and the constants for standard $k - \epsilon$ turbulence model are $c_\mu = 0.09$ and $c_{2\epsilon} = 1.92$. Now we have the source terms for mass balance, momentum equations and turbulence model. These sources are used in simulating 3D channel flow with 2D mesh. In addition, when modelling the behavior of plate heat exchangers we also need the energy equation for temperature modelling, which is derived in the next section.

2.2. Energy equation

As in previous derivations, we ignore the time derivative term that is the energy storage term. Other energy equation terms are the net rate of energy inflow by convection, plus the heat transfer rate across the boundary, plus the rate at which work is done on the fluid within the volume, plus the rate at which energy is produced within the volume. The most important factors in this study are convection with the flow and heat transfer through the lower and upper plates. Streamwise heat conduction within the fluid can be neglected for fluids with a Peclet number greater than 100 [11]. Thus, the depth-averaged energy equation can be written in the form

$$\nabla \cdot \left(\rho \bar{u} \left(e + \frac{1}{2} \bar{u}^2 \right) \right) = \nabla \cdot k \nabla T + \nabla \cdot (\bar{\tau} \cdot \bar{u}) - \frac{\rho}{D} \left(e + \frac{1}{2} \bar{u}^2 \right) \bar{u} \cdot \nabla D + \frac{-\dot{q}}{D} (1 + \gamma), \quad (12)$$

where γ is the local expansion coefficient of the plate area, e is the specific internal energy, k is the effective conductivity and T is the temperature. Due to the wavy surfaces, the effective heat transfer surface in 2D is taken into account by “expansion coefficient”

$$\gamma = A_1 + A_2, \quad (13)$$

where

$$A_1 = \frac{1}{2} \sqrt{1 + \left(\frac{\partial D}{\partial x} \right)^2} \sqrt{G} \sin \theta_1 \quad (14)$$

$$A_2 = \frac{1}{2} \sqrt{1 + \left(\frac{\partial D}{\partial y} \right)^2} \sqrt{G} \sin \theta_2 \quad (15)$$

and

$$\theta_1 = \arccos \left(\frac{1 + \frac{\partial D}{\partial x} \left(\frac{\partial D}{\partial x} + \frac{\partial D}{\partial y} \right)}{\sqrt{1 + \left(\frac{\partial D}{\partial x} \right)^2} \sqrt{G}} \right), \quad (16)$$

$$\theta_2 = \arccos \left(\frac{1 + \frac{\partial D}{\partial y} + \frac{\partial D}{\partial x} \frac{\partial D}{\partial y}}{\sqrt{1 + \left(\frac{\partial D}{\partial y} \right)^2} \sqrt{G}} \right), \quad (17)$$

where

$$G = 2 + \left(\frac{\partial D}{\partial x} + \frac{\partial D}{\partial y} \right)^2. \quad (18)$$

Note, that $\gamma = 1$ if the surfaces are horizontal plates so that $\frac{\partial D}{\partial x} = \frac{\partial D}{\partial y} = 0$. In addition, the heat flux \dot{q} in Eq. (12) needs to be handled with care. In [1] the law-of-the-wall for temperature consists of the linear law for the thermal conduction sublayer, where conduction is important, and the logarithmic law for the turbulent region. The law-of-the-wall has the following form for incompressible flow

$$T^* \equiv \frac{(T_w - T_p) \rho c_p c_\mu^{1/4} k_p^{1/2}}{\dot{q}} = \begin{cases} \text{Pr } y^* & (y^* < y_\tau^*) \\ \text{Pr}_\tau \left[\frac{1}{\kappa} \ln(Ey^*) + P \right] & (y^* > y_\tau^*) \end{cases}, \quad (19)$$

where

$$P = 9.24 \left[\left(\frac{\text{Pr}}{\text{Pr}_\tau} \right)^{3/4} - 1 \right] \cdot [1 + 0.28e^{-0.007\text{Pr}/\text{Pr}_\tau}], \quad (20)$$

k_p is the turbulent kinetic energy at point P , T_p is the temperature at point P , T_w is the wall temperature, C_p is the specific heat, Pr_τ is the turbulent Prandtl number ($=0.85$ at the wall), κ is the von Kármán

constant ($=0.4187$), E is the empirical constant ($=9.793$) and y_τ^* is the non-dimensional thermal sublayer thickness. The non-dimensional parameter y^* is

$$y^* \equiv \frac{\rho c_\mu^{1/4} k_p^{1/2} y_p}{\mu}, \quad (21)$$

where y_p is the distance from point P to the wall. It follows that the heat flux \dot{q} can be solved from Eq. (19).

2.3. Model validation

The fast modelling tool developed in this paper will be used to compare heat transfer and pressure losses for various heat exchanger designs. Thus, overall accuracy of the model is essential, but detailed point-wise velocities, pressures or turbulence quantities are not in our focus. First, 3D simulations are validated with experiments, and secondly, results of the depth-averaged model is compared to the 3D CFD predictions. Overall heat transfer coefficients and pressure losses are measured for one geometry and for three different flow rates. Measurements and 3D simulations are compared in Fig. 1. As seen in the figure, the pressure drop as a function of the heat transfer coefficient can be predicted with the 3D CFD model accurately enough. Thus, the starting point of our modelling work, that is, the full 3D model including the steady-state $k - \epsilon$ model, is reasonable.

The depth-averaged continuity and momentum equations can be mathematically derived from the 3D equations, but depth-averaging of the turbulence model includes closure problems and requires simplifications. It leads to additional source terms for turbulence kinetic energy and its dissipation which are adopted from [10]. As concluded in [10], Froude number has to be at least 10 to get satisfactory results with the depth-averaged model when the surfaces of flow channel are smooth. The limitation exists because buoyancy effects cannot be taken into account by depth-averaged model. This condition is satisfied in the present study as Froude number is in all simulations at least 50. Thus, the buoyancy effects are insignificant.

In the light of these validations, the depth-averaged model is sufficiently accurate for overall heat transfer and pressure loss calculations, but one should be cautious about using the depth-averaged model for detailed predictions of the point-wise velocity components, temperature and other variables. It is also worth to remember, that after using the fast depth-averaged model for

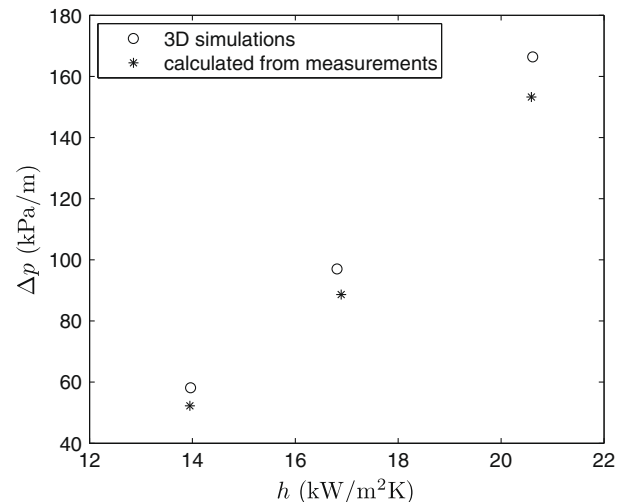


Fig. 1. Pressure drop as a function of heat transfer coefficient for three different flow rates.

design examinations, all the most potential designs can be evaluated with the full 3D model with higher accuracy.

2.4. The simulation setup

In the present study we have only one flow channel where cold water flows. Both channel geometries, 3D and 2D for fast modeling, are illustrated in Fig. 2. The water is heated by the plates above and beneath. Inflow water is set to be at a temperature of 323 K and plates at a constant temperature of 335 K. The used boundary condition for inflow is velocity inlet and outlet is set to be at a constant pressure of 0 Pa.

3. Results

In the previous section we presented 2D flow and energy equations for a 3D channel flow. The comparison between 2D and 3D simulation results of the pressure drop and water heating with different geometries verify the usability of the 2D model in the product development process. The 2D approach predicts well both flow behavior and heating. This can be seen in Figs. 3 and 4 where path lines and fluid temperature are shown for 2D and 3D geometries with a corrugation angle of 55° and constant plate temperature of 335 K. It can be seen that in the 2D geometry water circulates around the junctions and heats up, so the hot spots of water are identified, as in the 3D geometry.

Our model predicts well the change in pressure drop and temperature as a function of the corrugation angle and the corrugation length. Profiles of the pressure drop and the temperature change as a function of the corrugation angle are presented in Figs. 5 and 6, and as a function of the corrugation length in Figs. 7 and 8. The normalized pressure drop and temperature change are determined by dividing the absolute values by the average values

$$\Delta p^* = \frac{\Delta p}{\overline{\Delta p}}, \tag{22}$$

$$\Delta T^* = \frac{\Delta T}{\overline{\Delta T}}. \tag{23}$$

For both quantities, dependencies on the corrugation angle and on the corrugation length are accurately predicted in 2D.

For more extensive information about the efficiency of heat exchangers as a function of the corrugation angle β and the corrugation length s we simulated 30 different geometries, where the corrugation angle and the corrugation length varied between 55°–60° and 8–12 mm, respectively. The resulted pressure drops and temperature changes are illustrated as interpolation surfaces in Figs. 9 and 10. From these visualizations it is easy to see that while the temperature change increases the pressure drop increases too, in other words, the temperature change is highly proportional to the pressure drop. In addition, the temperature change

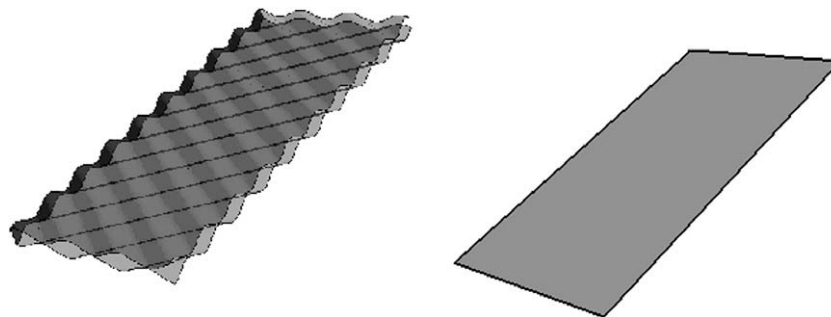


Fig. 2. 3D channel geometry (left) and 2D channel geometry (right).

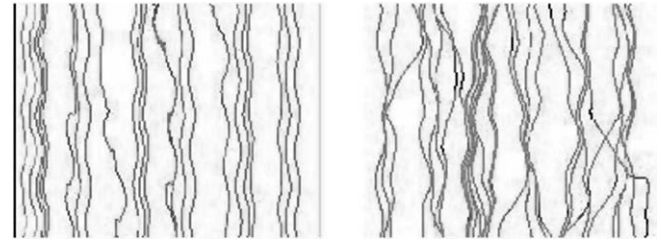


Fig. 3. Path lines in the plate gap for 2D (left) and 3D (right) geometries. (Only part of the modelled channels are shown.)

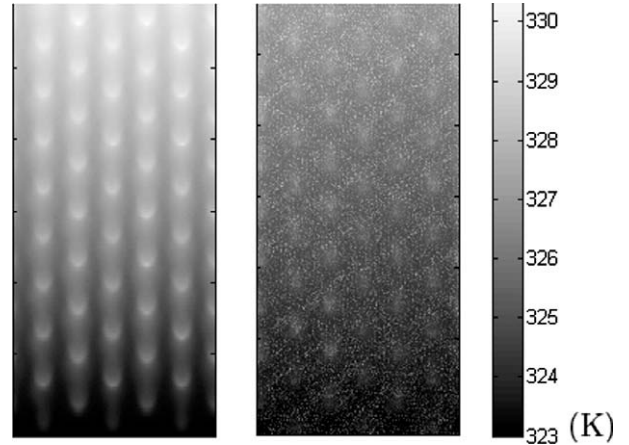


Fig. 4. Water heating in the plate gap for 2D (left) and 3D (right) geometries.

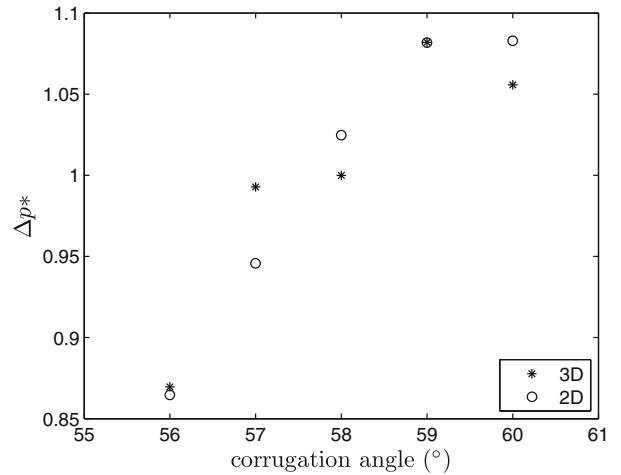


Fig. 5. Normalized pressure drop as a function of the corrugation angle.

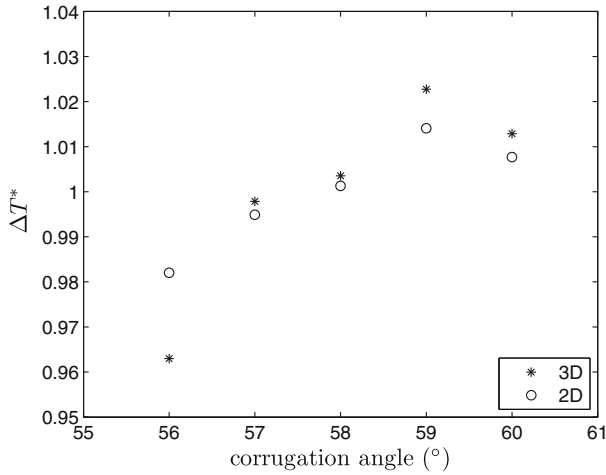


Fig. 6. Normalized temperature change as a function of the corrugation angle.

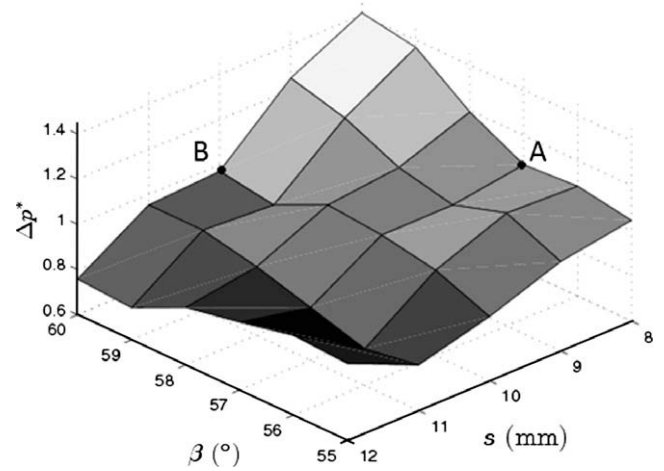


Fig. 9. Normalized pressure drop as functions of the corrugation angle and the corrugation length.

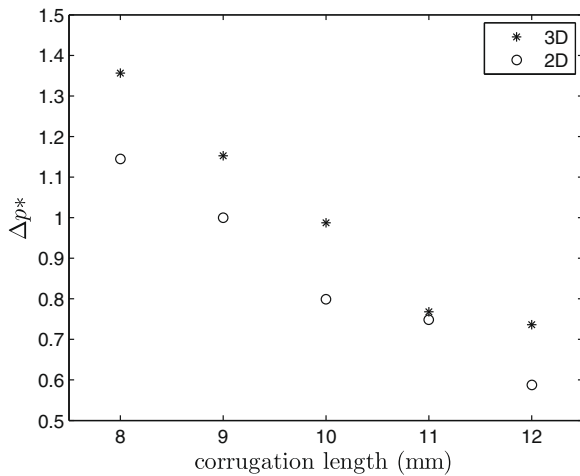


Fig. 7. Normalized pressure drop as a function of the corrugation length.

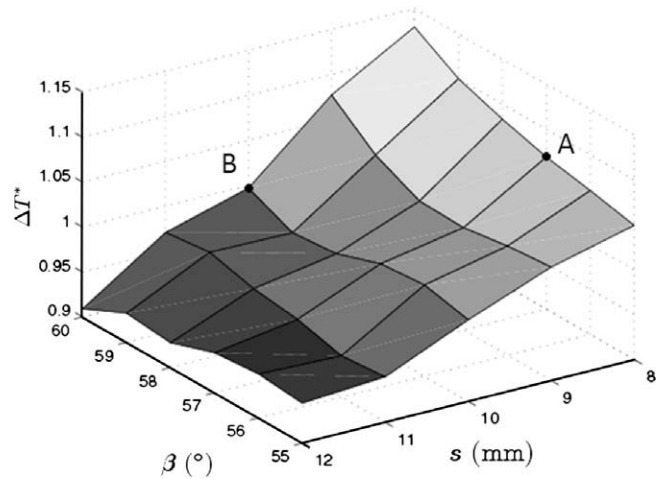


Fig. 10. Normalized temperature change as functions of the corrugation angle and the corrugation length.

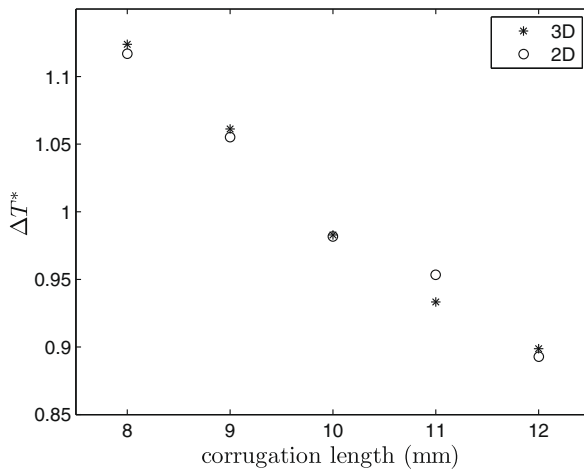


Fig. 8. Normalized temperature change as a function of the corrugation length.

seems not to be as sensitive to geometrical modifications as the pressure drop. Thus, it is hard to find one geometry that provides low pressure drop and high temperature change at the same time. However, for the certain acceptable pressure drop level, optimal corrugation angle and length can be found. For example, the solu-

tion A in the Figs. 9 and 10 is interesting, because the pressure drop is relatively low and the heat transfer is high compared to the solution B.

4. Conclusions

The design of the plate surface is the key issue in the product development of heat exchangers, when maximizing the heat transfer. It also affects the head loss, which, in turn, should be kept reasonably small. CFD is a very promising tool to study heat exchangers, but still one major challenge is the complex 3D geometry of heat exchangers. The pre-processing, i.e., modelling the detailed geometry and generating a good quality mesh, is extremely time consuming. Furthermore, the actual simulation for a 3D heat exchanger takes hours with an ordinary PC. Therefore, the development of faster modelling methods is of utmost importance in order to produce tools for real design work. Replacing the full 3D flow and energy equations by the depth-averaged equations makes it possible to save both human and CPU time. The complex 3D geometry need not be modelled nor discretized in the pre-processing state: instead, the plate gap is only described with source terms in the depth-averaged equations, which are then solved in a very simple and fixed 2D domain. The method is also very fast from the point of view of a computational time, since obtaining the

solution for one 2D geometry takes only few minutes. Even though the depth-averaged equations lose some 3D flow structures, they are capable of presenting the general flow behavior with surprisingly good accuracy. Further, they speed up the design process and help in finding the most interesting geometries, which can be examined with 3D modelling and experimental pilot tests in more detail. The method introduced in this paper gives a good basis for the further development of the fast and efficient modelling of heat exchangers.

Acknowledgements

This research has been accomplished in close co-operation with and financially supported by Danfoss LPM. We thank especially Pertti Ruotsalainen, Antti Tapanainen, and Jukka Hyvärinen for providing us with practical information of the heat exchanger design process.

References

- [1] FLUENT 6.2 User's Guide.
- [2] M.K. Bassiouny, H. Martin, Flow distribution and pressure drop in plate heat exchangers – i, *Chem. Eng. Sci.* 39 (1984) 693–700.
- [3] M.K. Bassiouny, H. Martin, Flow distribution and pressure drop in plate heat exchangers – ii, *Chem. Eng. Sci.* 39 (1984) 701–704.
- [4] P.R. Bobbili, B. Sunden, S.K. Das, An experimental investigation of the port to channel flow and pressure distribution of the smaller and larger plate package heat exchangers, in: R.K. Shah, M. Ishizuka, T.M. Rudy, V.V. Wadekar (Eds.), *Enhanced, Compact and Ultra-Compact Heat Exchangers: Science, Engineering and Technology*, 2005, pp. 200–207.
- [5] P.R. Bobbili, B. Sunden, S.K. Das, An experimental investigation of the port flow maldistribution in small and large plate package heat exchangers, *Appl. Thermal Eng.* 26 (2006) 1919–1926.
- [6] F.C.C. Galeazzo, R.Y. Miura, J.A.W. Gut, C.C. Tadini, Experimental and numerical heat transfer in a plate heat exchanger, *Chem. Eng. Sci.* 61 (2006) 7133–7138.
- [7] Y. Islamoglu, C. Parmaksizoglu, The effect of channel height on the enhanced heat transfer characteristics in a corrugated heat exchanger channel, *Appl. Thermal Eng.* 23 (2003) 979–987.
- [8] A.G. Kanaris, A.A. Mouza, S.V. Paras, Flow and heat transfer in narrow channels with corrugated walls a cfd code application, *Chem. Eng. Res. Des.* 83 (A5) (2005) 460–468.
- [9] H.M. Metwally, R.M. Manglik, Enhanced heat transfer due to curvature-induced lateral vortices in laminar flows in sinusoidal corrugated-plate channels, *Int. J. Heat Mass Transfer* 47 (2004) 2283–2292.
- [10] A.K. Rastogi, W. Rodi, Prediction of heat and mass transfer in open channels, *J. Hydraul. Div.* 104 (HY3) (1978) 397–420.
- [11] W.Q. Tao, Z.Y. Guo, B.X. Wang, Field synergy principle for enhancing convective heat transfer – its extensions and numerical verifications, *Int. J. Heat Mass Transfer* 45 (2002) 3849–3856.